Molecular Therapy
Methods & Clinical Development
Original Article

In vivo CRISPR-Cas9 inhibition of hepatic LDH as treatment of primary hyperoxaluria

Rebeca Martinez-Turrillas,[1,6,9] Angel Martin-Mallo,[2,6,9] Saray Rodriguez-Diaz,[1,6] Natalia Zapata-Linares,[1,8] Paula Rodriguez-Marquez,[2,6] Patxi San Martin-Uriz,[2,6] Amaia Vilas-Zornoza,[2,6,7] María E. Calleja-Cervantes,[2,6] Eduardo Salido,[3,4] Felipe Prosper,[1,2,5,6,7] and Juan R. Rodriguez-Madoz[1,2,6,7]

[1]Regenerative Medicine Program, CIMA Universidad de Navarra, 31008 Pamplona, Spain; [2]Hemato-Oncology Program, CIMA Universidad de Navarra, 31008 Pamplona, Spain; [3]Pathology Department, Hospital Universitario Canarias, Universidad La Laguna, 38320 Tenerife, Spain; [4]Centro de Investigación Biomédica en Red de Enfermedades Raras (CIBERER), 28029 Madrid, Spain; [5]Cell Therapy Area, Clinica Universidad de Navarra (CUN), 31008 Pamplona, Spain; [6]Instituto de Investigación Sanitaria de Navarra (IdiSNA), 31008 Pamplona, Spain; [7]Centro de Investigación Biomédica en Red de Cáncer (CIBERONC), 28029 Madrid, Spain

Genome-editing strategies, especially CRISPR-Cas9 systems, have substantially increased the efficiency of innovative therapeutic approaches for monogenic diseases such as primary hyperoxalurias (PHs). We have previously demonstrated that inhibition of glycolate oxidase using CRISPR-Cas9 systems represents a promising therapeutic option for PH type I (PH1). Here, we extended our work evaluating the efficacy of liver-specific inhibition of lactate dehydrogenase (LDH), a key enzyme responsible for converting glyoxylate to oxalate; this strategy would not be limited to PH1, being applicable to other PH subtypes. In this work, we demonstrate a liver-specific inhibition of LDH that resulted in a drastic reduction of LDH levels in the liver of PH1 and PH3 mice after a single-dose delivery of AAV8 vectors expressing the CRISPR-Cas9 system, resulting in reduced urine oxalate levels and kidney damage without signs of toxicity. Deep sequencing analysis revealed that this approach was safe and specific, with no off-targets detected in the liver of treated animals and no on-target/off-tissue events. Altogether, our data provide evidence that *in vivo* genome editing using CRISPR-Cas9 systems would represent a valuable tool for improved therapeutic approaches for PH.

INTRODUCTION

Primary hyperoxalurias (PH) are a group of autosomal recessive metabolic disorders caused by oxalate overproduction as a result of genetic defects in enzymes involved in glyoxylate metabolism.[1,2] In PH patients, overproduction of oxalate, an end-product of glyoxylate metabolism, causes precipitation of calcium oxalate (CaOx) crystals in the kidney that results in urolithiasis, nephrocalcinosis, and progression to end-stage renal disease and renal failure.[1,2] There are three forms of PH (PH type I [PH1], PH2, and PH3), which are caused by mutations in alanine-glyoxylate aminotransferase (AGT), glyoxylate reductase/hydroxypyruvate reductase (GRHPR), and 4-hydroxy-2-oxoglutarate aldolase 1 (HOGA1), respectively,[3–5] with PH1 being the most common and severe subtype (around 70%–80% of all PH patients). Glyoxylate is converted into glycine, glycolate, or oxalate by AGT, GRHPR, or lactate dehydrogenase (LDH), respectively. Thus, reduced activity of AGT and/or GRHPR leads to increased accumulation of glyoxylate and subsequent overproduction of oxalate (Figure S1).[1,2]

Existing treatments aim to preserve renal function as long as possible by increasing fluid intake, dialysis, or administration of oxalate crystal inhibitors.[6] However, these treatments are insufficient and once renal function is compromised, combined kidney and liver transplantation is the only lifesaving option.[7] Currently, several molecular approaches are under investigation, including oxalate-degrading enzymes, AGT mistargeting correction (applicable only to patients with specific mutations), as well as gene and cell therapies.[8–11] Small interfering RNA (siRNA)-mediated silencing of specific enzymes of the glyoxylate metabolism are attractive strategies that have demonstrated reduction of oxalate excretion in animal models of PH1,[12,13] as well as in clinical trials (ILLUMINATE studies),[14] leading to the approval of lumasiran for the treatment of PH1. Another interesting target is LDH, an enzyme that plays a critical role in hepatic oxalate production in PH.[15] LDH is tetrameric protein composed by combinations of M and H subunits (encoded by LDHA and LDHB, respectively), with LDH5 (4M subunits) being the major isozyme of the liver.[16] The absence of any compromised liver function in LDHA-deficient patients (reviewed in Ariceta et al.[17]) makes LDHA an ideal target. RNAi-mediated liver-specific knockdown of LDHA has been reported[18] in several animal models of PH, providing evidence of oxalate reduction with no apparent adverse effects in non-hepatic tissues. Moreover, the recently completed clinical trial PHYOX1 (ClinicalTrials.gov: NCT03392896) evaluating Nedosiran, an investigational RNAi therapy targeting LDHA, demonstrated some evidence of pharmacodynamic effect, in both PH1 and PH2 subpopulations,

Received 20 February 2021; accepted 14 March 2022;
https://doi.org/10.1016/j.omtm.2022.03.006.

[8]Present address: Sorbonne Université, INSERM UMR-S 938, Center de Recherche Saint-Antoine (CRSA), Paris, France

[9]These authors contributed equally

Correspondence: Juan R. Rodriguez-Madoz, Regenerative Medicine Program, CIMA Universidad de Navarra, 31008 Pamplona, Spain.
E-mail: jrrodriguez@unav.es

with acceptable safety.[19] However, siRNAs or small molecules have several limitations, such as the requirement of multiple administrations for long-term effect or the incomplete inhibition of the target enzyme.

The latest advances in CRISPR-Cas9 systems[20–22] provide useful tools for the development of improved therapies, with some of them already under evaluation in human trials.[23–25] The CRISPR-Cas9 system, composed by the Cas9 nuclease and a programmable guide RNA, can be exploited for efficient gene inactivation. In a previous work, we showed that targeting the *Hao1* gene, coding for glycolate oxidase (GO), using AAV-based CRISPR-Cas9 systems in a mouse model of PH1 resulted in long-term specific inhibition of hepatic GO, leading to the reduction of urine oxalate excretion to normal levels and preventing nephrocalcinosis with an absence of toxic effects.[26] We hypothesize that *in vivo* CRISPR-Cas9 strategies could be applicable to other PH forms, and in this work, we explored its usefulness evaluating the efficacy of targeting the liver *Ldha* gene in preclinical models of PH1 and PH3. Our results showed that a single administration of the therapeutic vector resulted in liver-specific long-term LDH inhibition, reduced urine oxalate levels, and prevented kidney damage without signs of toxicity in both animal models.

RESULTS

Efficient *in vivo* inhibition of hepatic LDH using CRISPR-Cas9 systems in *Agxt1*$^{-/-}$ mice

In order to evaluate CRISPR-Cas9-mediated LDH inhibition as a treatment of PH1, we designed and selected four different single guide RNAs (sgRNAs) targeting the murine *Ldha* gene (exonic regions) based on their location and the predicted on-target/off-target efficiency (Table S1). Cleavage efficiency was evaluated *in vitro* by TIDE[27] after transfection of *Staphylococcus aureus* Cas9 (SaCas9) and sgRNA ribonucleoprotein (RNP) complexes in AML12 and Hepa1-6 cell lines, selecting mLdha.ex5.sgRNA2 for further studies (Figure S1). For *in vivo* LDH inhibition, the selected *Ldha*-targeting sgRNA was delivered to the liver of *Agxt1*$^{-/-}$ (PH1) mice using a single AAV8 vector expressing the sgRNA under a U6 promoter and SaCas9 under the liver-specific thyroxine binding globulin (TBG) promoter[28] in order to restrict genome editing to hepatocytes. *In vivo* cleavage efficiency was evaluated in 10- to 14-week-old PH1 male mice[29] after intravenous administration of AAV8-SaCas9-*Ldha*-sgRNA (sgRNA) at a dose of 5×10^{12} vg/kg. Groups of animals receiving the same dose of AAV8-SaCas9 without sgRNA (Cas9) and PBS, as well as wild-type (WT) animals, were used as controls. Mice were sacrificed 8 weeks (short term) and 6 months (long term) after treatment. We evaluated vector genome copies and expression of SaCas9 in different organs, observing a predominant hepatic viral transduction with a restricted Cas9 expression to the liver (Figure S1). Cleavage efficacy and indel frequencies were measured by TIDE, detecting an average of 41.81% (short term) and 47.98% (long term) of indels only in the livers of PH1 animals that received the gRNA vector (Figure 1A). Moreover, we observed reduced *Ldha* transcription levels in these animals receiving the therapeutic vector (Figure 1B). In accordance, a dramatic reduction of LDH protein expression was observed in the liver of treated animals after western blot analysis (with >95% of reduction) (Figures 1C and S1), being almost below the level of detection. Furthermore, only a reduced and isolated number of LDHA-positive cells were detected in sgRNA-treated animals by immunohistochemical analysis, while control animals had a homogeneous staining of the hepatocytes (Figure 1D).

To further characterize the efficiency of genome editing and the variant distribution in the liver of treated animals, we amplified the *Ldha*-targeted locus by PCR and analyzed it by next-generation sequencing (NGS). Indel averages of 52.96% (short term) and 58.17% (long term) were observed in the liver of treated animals (Table 1; Figure S2), results that confirmed previous observations with TIDE. The most common mutations were small deletions <10 bp (>70% deletions < 3 bp), targeting coding or splice-site regions, with >80% of indels occurring around positions +1 or +2 relative to the cleavage site (Figures 2 and S2). More importantly, these modifications introduced frameshift mutations in both PH models (Figure 2B), which explained the reduction observed at protein levels (Figures 1C and 1D).

CRISPR-Cas9-mediated LDH inhibition induces a long-term therapeutic effect

We further evaluated both short-term and long-term therapeutic efficacy of CRISPR-Cas9-mediated LDH inhibition as treatment for PH1. Thus, PH1 male mice were treated with therapeutic vector (and controls) as described above. No significant differences were observed in urine oxalate and glycolate levels measured at different time points after AAV administration between sgRNA-treated animals and control groups (Cas9 and PBS) (Figures 3A and S3). To induce oxaluria, we overload the glyoxylate pathway using ethylene glycol (EG), a precursor of glyoxylate that increases oxalate production.[9] Then therapeutic efficacy was analyzed in PH1 animals challenged during 7 consecutive days with 0.5% EG in drinking water. In both experimental conditions (short and long term), urine oxalate levels were significantly lower at day 7 after challenge in the animals that received treatment with sgRNA compared with control groups (Cas9 and PBS) and, more interestingly, presented similar levels to that observed in WT animals (Figure 3B), indicating the therapeutic efficacy of CRISPR-Cas9-mediated LDH inhibition. As expected, glycolate levels increased after EG challenge, especially in the group of animals treated with sgRNA targeting *Ldha*, although no statistical differences were observed between groups at day 3 or 7 of continuous EG challenge (Figure S3). No difference in water intake or urine volume was observed, indicating a homogeneous EG challenge (Figure S3).

Previous studies have shown that glyoxylate pathway overload is well tolerated without any apparent toxic effect in WT animals, while an increased weight loss is observed in PH animals.[26] Interestingly, reduction in body weight loss was observed during the challenge, in animals treated with the therapeutic vector, indicating that

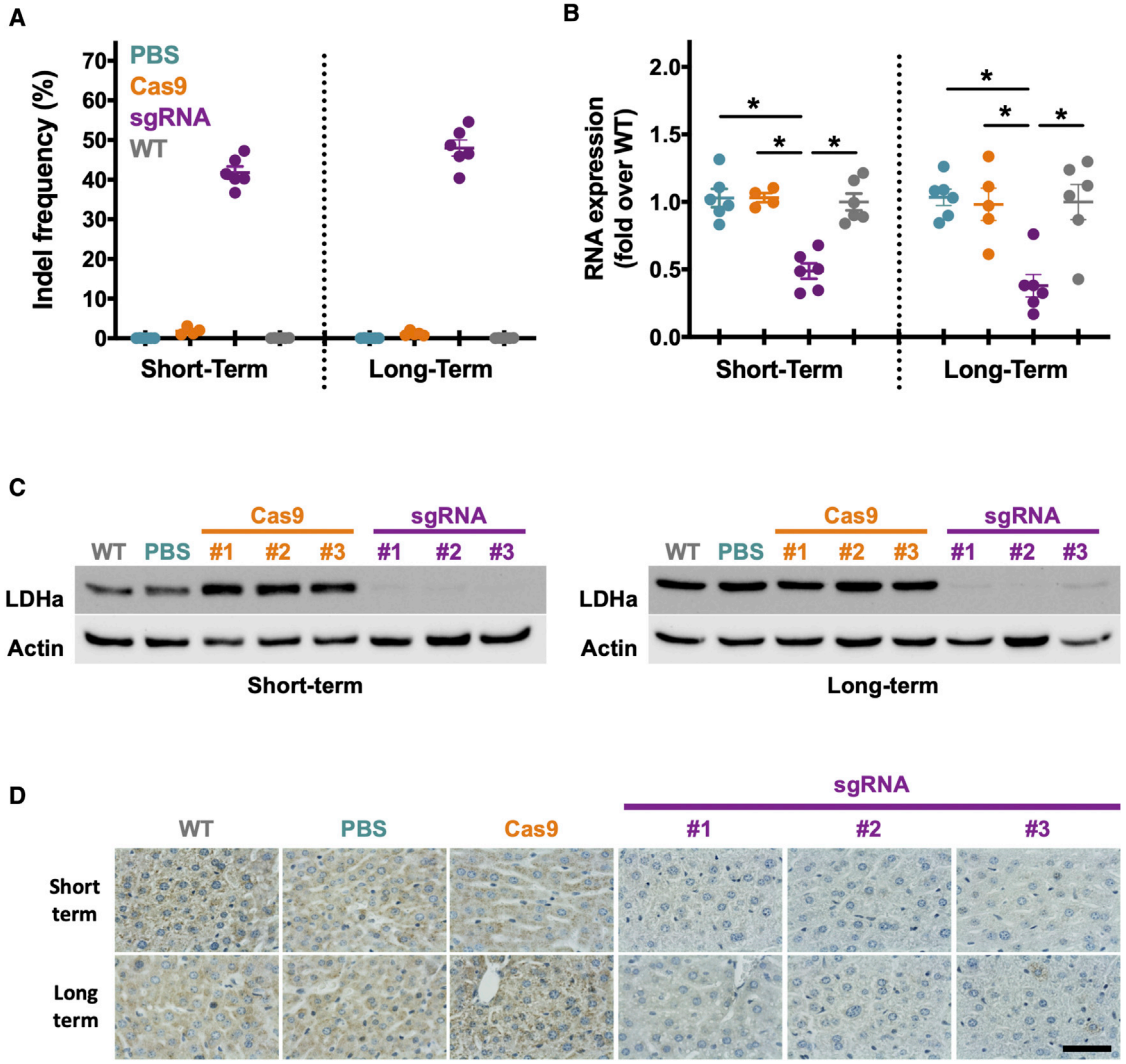

Figure 1. Efficient *in vivo* inhibition of hepatic LDH using CRISPR-Cas9 systems in *Agxt1*$^{-/-}$ mice

Groups of 10- to 14-week-old PH1 animals were treated with PBS (n = 6), Cas9 (n = 4/5), and sgRNA (n = 6) and analyzed 8 weeks (short term) or 6 months (long term) after the administration of the treatment. A group of WT animals (n = 6) was included as control. (A) Editing efficiency measured by TIDE. (B) Quantification of *Ldha* mRNA expression by quantitative real-time PCR. (C) Western blot (WB) analysis of LDH protein levels in representative animals treated with PBS, Cas9, and sgRNA. Actin was used as control. (D) Representative immunohistochemistry (IHC) images of the liver stained for LDHA of WT and PH1 animals treated with PBS, Cas9, and sgRNA. Scale bar: 100 μm. Kruskal-Wallis statistical test was used to evaluate differences between groups. *$p < 0.05$.

CRISPR-Cas9-mediated LDH inhibition also ameliorates this detrimental effect (Figure 3C). *Agxt1*$^{-/-}$ mice, challenged with EG,[29] develop variable degrees of kidney CaOx deposits. Thus, we also analyzed the capacity of our treatment to prevent kidney damage. Groups of PH1 animals were treated as described above with the therapeutic vector, including PBS, Cas9, and WT groups as control, and challenged with EG for a longer period of time (15 days). Then, kidney histology was analyzed 8 weeks (short term) or 6 months (long term) after AAV administration. We observed a high degree of kidney damage in control animals (PBS and Cas9), while animals treated with the therapeutic vector displayed a normal histology similar to the WT group (Figures 3D and S3). Moreover, control animals showed a high degree of CaOx deposits in their kidneys, an effect that was prevented in most of the PH1 mice treated with the therapeutic vectors, with only some residual CaOx deposits (Figure 3E). These results clearly indicate that our therapeutic strategy was able to reduce urine oxalate levels and also to protect from kidney damage and CaOx deposits caused by prolonged hyperoxaluria in a PH1 mouse model.

Higher doses of therapeutic vector do not improve therapeutic efficacy

In order to evaluate whether the therapeutic efficacy was improved by increasing the dose of the AAV8 vector, we intravenously treated

Table 1. Variants (%) in on-target and off-target sites

Experiment	Group	ONT	OFT #1	OFT #2	OFT #3	OFT #4	OFT #5
Short term	PBS (n = 1)	0.05	0.12	0.05	0.07	0.12	0.07
	sgRNA (n = 6)	52.96	0.10	0.09	0.09	0.09	0.07
Long term	PBS (n = 1)	0.15	0.10	0.12	0.09	0.11	0.13
	sgRNA (n = 6)	58.17	0.08	0.09	0.10	0.10	0.07
High dose	PBS (n = 1)	0.09	0.12	0.14	0.11	0.18	0.08
	sgRNA (n = 6)	57.44	0.10	0.09	0.12	0.12	0.06
PH3	PBS (n = 1)	0.15	0.11	0.11	0.17	0.14	0.06
	sgRNA (n = 8)	53.20	0.11	0.08	0.10	0.11	0.07

OFT, off-target; ONT, on-target.

groups of 10- to 14-week-old PH1 male mice with 10^{14} vg/kg AAV8-SaCas9-*Ldha*-sgRNA (sgRNA). Animals receiving the same dose of vector without sgRNA (Cas9), as well as PBS-treated and WT animals, were used as controls. Compared with previous experiments (short or long term), a similar genome-editing efficiency and variant distribution was observed in the liver of treated animals 8 weeks after vector administration (Figure S4). Increasing the dose, we observed a slightly higher frequency of indel generation (51.76%) that resulted again in a strong reduction of *Ldha* transcription levels and LDH protein expression. However, the effect of LDH inhibition with higher doses of therapeutic vector on urine oxalate levels after 7-day EG challenge was not dramatically improved, with significant lower levels compared with control only at day 7, as observed previously (Figure S4). Looking at the body weight loss, we observed a slightly better performance of treated animals, with significantly lower reduction of the weight compared with controls (PBS and Cas9) and being closer to WT (Figure S4). In summary, these results indicate that increasing the dose of the AAV therapeutic product does not significantly increase the efficacy.

Therapeutic efficacy of CRISPR-Cas9-mediated LDH inhibition in *Hoga1*$^{-/-}$ mice

In order to evaluate our CRISPR-Cas9-mediated LDH inhibition strategy as treatment of other PH subtypes, we evaluated the long-term therapeutic efficacy in *Hoga1*$^{-/-}$ mice, a model of PH3.[30] Thus, groups of 10- to 14-week-old PH3 male mice were treated as described above (sgRNA, Cas9, PBS, and a group of WT mice as control). For this long-term experiment, mice were sacrificed 20 weeks after treatment, and again vector genome copies and SaCas9 expression were analyzed, showing a predominant hepatic transduction with restricted Cas9 expression to the liver (Figure S5). Compared with long-term experiment in PH1, cleavage efficacy and indel frequencies in the livers of PH3 animals that received the gRNA vector were reduced (average of 39.04%) (Figure 4A). Nevertheless, variant distribution was similar to previously observed in PH1 with small deletions <10 bp at positions +1/+2 of the cleavage site, indicating that these characteristics are intrinsic to sgRNA (Figure S5). Importantly, despite this slightly reduced cleavage efficacy, *Ldha* transcription levels and LDH protein expression were significantly reduced (Figures 4B and 4C), indicating proper inhibition of LDH in the liver. To evaluate the therapeutic efficacy of CRISPR-Cas9-mediated LDH inhibition in the PH3 model, we challenged treated animals 20 weeks after AAV administration for 7 consecutive days. For PH3 mice, the challenge was performed with 0.25 M hydroxyproline (HP) in drinking water, a condition that showed more reproducible oxalate induction in male mice (Figure S6). Oxalate production was moderately reduced in PH3 animals compared with EG induction in PH1, probably because of a lower water intake during the challenge, although no differences in water intake or urine volume were observed between the groups, indicating a homogeneous challenge (Figure S7). The quantification of urine oxalate after HP challenge showed significantly lower levels at day 7 in the animals that received the treatment, being similar to that observed in WT animals (Figure 4D). Finally, we observed a reduction in body weight loss in these animals treated with the therapeutic vector (Figure 4E), indicating that our CRISPR-Cas9-based therapeutic approach was also effective in PH3. In contrast with the results observed in the PH1 model, no kidney damage was observed in any of the groups of PH3 mice (not even controls) challenged during 15 days with HP, probably because of the lower frequency of oxalate stones and systemic oxalosis observed in PH3 patients.[31] Together, our data suggest that inhibition of LDH with CRISPR-Cas9 systems could be considered an efficient therapy for different types of PH.

Safety of CRISPR-Cas9-mediated LDH inhibition

One of the potential issues associated to CRISPR-Cas9 therapies would be the genotoxicity caused by non-specific cleavage of the genome. Thus, we evaluated cleavage specificity performing deep sequencing of the on-target site together with the top 5 off-target regions (Table S2) for the selected sgRNAs in all the experimental conditions evaluated (short-term, long-term, high-dose, and PH3 experiments). Our results showed that frequencies at the off-target regions (OFT1–5) were similar to those observed in control animals (usually <0.1%) (Table 1; Figure S8). The on-target site was also analyzed in different tissues of PH1 animals from the long-term experiment (on-target/off-tissue effect). Again, the frequencies observed were similar to the ones observed in control mice (Table S3; Figure S8), corroborating the hepato-specificity

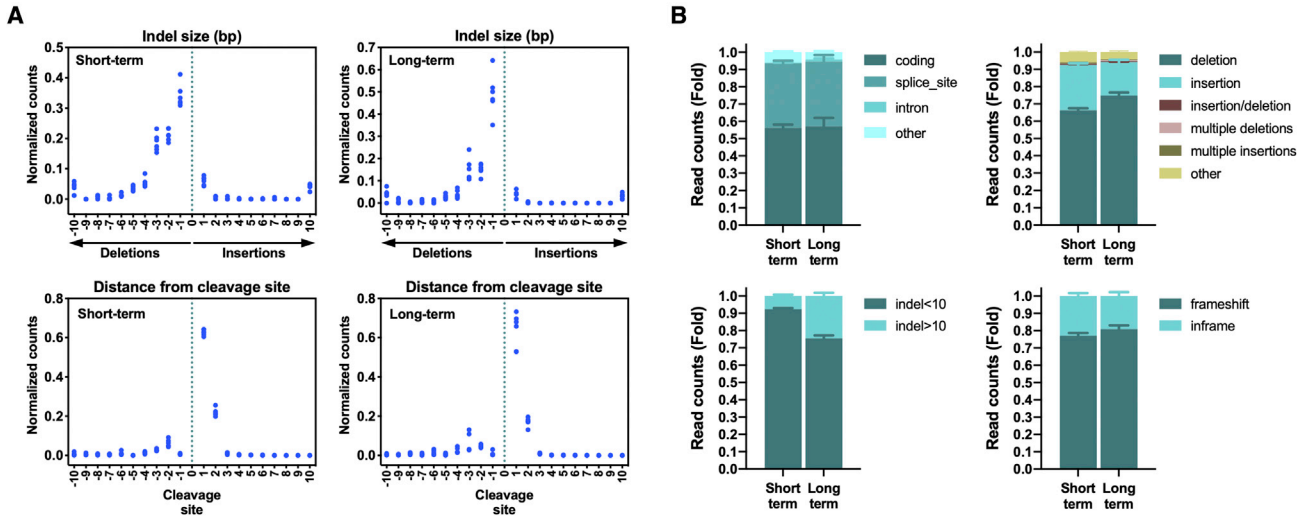

Figure 2. Characterization of CRISPR-Cas9-mediated LDH editing in *Agxt*$^{-/-}$ mice

Analysis performed in 10- to 14-week-old PH1 animals treated with PBS (n = 6), Cas9 (n = 4/5), and sgRNA (n = 6) and in WT animals (n = 6) at 8 weeks (short term) or 6 months (long term) after administration of the treatment. (A) Frequency distribution of indel size (up) and distance from cleavage site (bottom) in animals treated with sgRNA. (B) Indel characterization according to their localization, type, size, and frameshift potential in animals treated with sgRNA.

of our vector. Another safety issue recently described for this type of therapy is the possible AAV integration into the sgRNA targeted site.[32] Despite that most common mutations of our selected sgRNA were small deletions under 10 bp, we further analyzed AAV integration events into the *Ldha*-targeted region. We observed that >50% of the insertions >10 bp included AAV sequences corresponding to the ITR regions (Figure S8; Table S4). The AAV-integrated sequences increased up to 73.83% of the insertions >10 bp when high AAV doses were used, suggesting a correlation between the AAV dose and the integration events. However, in total, these AAV insertions represented only 2%–5% of total indels (Table S4), suggesting that our therapeutic approach targeting *Ldha* would be safe and tissue specific with no significant off-target effect *in vivo*. Furthermore, we performed histopathology analysis of liver sections and measured serum transaminase levels to evaluate the potential hepatotoxicity of the treatment. We observed a normal histology in the liver of animals treated with the therapeutic vector, as well as normal levels of aspartate aminotransferase (AST) and alanine aminotransaminase (ALT) (Figure 5). Having in mind that a patient's safety cannot be fully predicted, our data suggest that the specific inhibition of LDH in the liver, using CRISPR-Cas9 therapeutic approaches, would be a safe option to treat PH.

DISCUSSION

Advances in CRISPR-Cas9 technology have boosted the development of innovative approaches for many inherited disorders, as well as other pathological conditions, showing promising outcomes in animal models.[33–38] More importantly, recent studies in human trials have shown very positive and optimistic results of CRISPR-Cas9-based approaches.[23–25] In this study, we have extended our previous work based on CRISPR-Cas9-mediated gene editing as treatment for PH1, for the development of improved therapeutic strategies that would be applicable for other PH subtypes. For that purpose, we have redirected the CRISPR-Cas9 system against the hepatic isoform of LDH, a key enzyme responsible for converting glyoxylate to oxalate. Several studies indicate that LDH inhibition is a promising therapy for several subtypes of PH using siRNAs or even CRISPR-Cas9 strategies,[18,39] and recent results from the PHYOX1 trial evaluating Nedosiran showed positive results at least for PH1. However, our therapeutic strategy to inhibit LHD would help to overcome some of the limitations observed with siRNA approaches. In particular, our approach would avoid the requirement of multiple administrations for long-term effect,[14,18,19] because of the transient effect of siRNAs, which would represent a clear benefit in the quality of life of patients and their families.

We have demonstrated that a single dose of an AAV8 vector carrying the SaCas9 and a sgRNA targeting LDH, administered into the livers of *Agxt1*$^{-/-}$ and *Hoga1*$^{-/-}$ mice, models of PH1 and PH3, respectively, efficiently and specifically induced indels in the target gene (*Ldha*), resulting in a sustained and highly significant reduction of LDH protein. TIDE and NGS analysis of the liver of treated animals revealed an average of 40%–50% of indels, while the LHD protein remained almost undetectable. This apparent discrepancy between indel frequency and protein disappearance has been previously observed, and it is due to the specific and restricted SaCas9 expression to the hepatocytes.[26,28] Because indel analysis is performed using whole liver samples, the non-edited DNA, from other cell types, masks the cleavage efficiency that is increased when measured in purified hepatocytes, a fact already demonstrated by our group.[26]

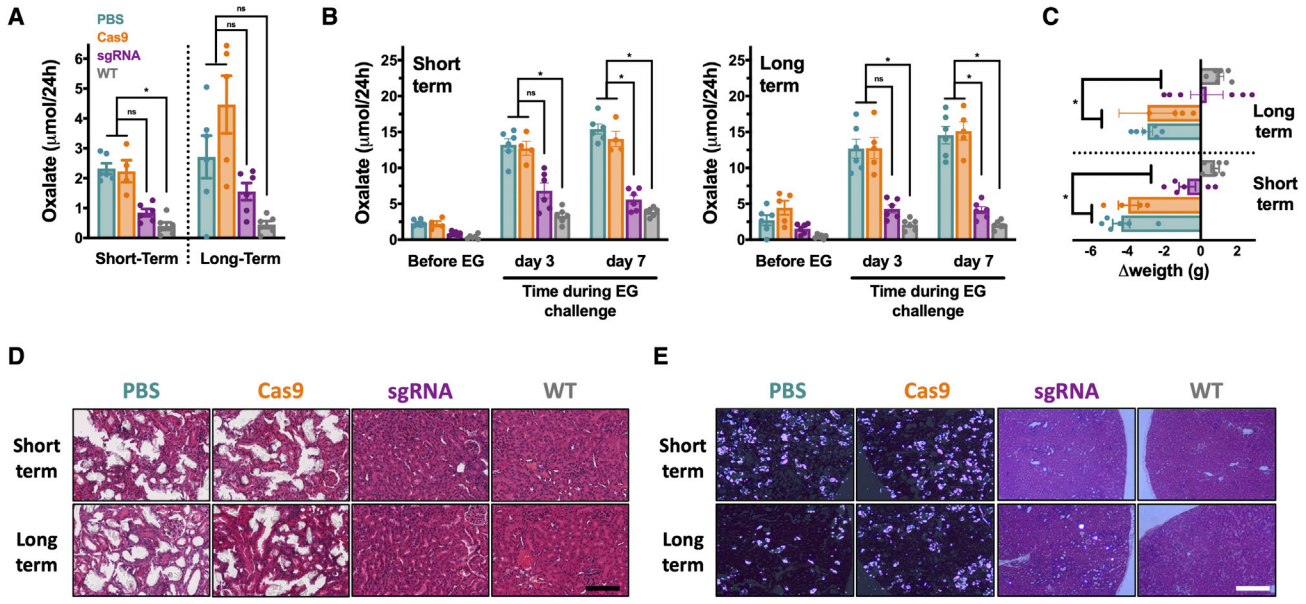

Figure 3. Therapeutic efficacy of CRISPR-Cas9-mediated LDH inhibition in *Agxt1*$^{-/-}$ mice

Analysis performed in 10- to 14-week-old PH1 animals treated with PBS (n = 6), Cas9 (n = 4/5), and sgRNA (n = 6) and in WT animals (n = 6) at 8 weeks (short term) or 6 months (long term) after administration of the treatment. (A) Quantification of basal urine levels of oxalate (µmol/24 h) in the different groups of treatment. (B) Quantification of urine oxalate levels (µmol/24 h) before and on days 3 and 7 of EG challenge in the different groups of treatment. (C) Weight change of the animals after 1 week of EG challenge in the different groups of treatment. (D) Histological analysis of renal damage in representative kidneys of animals from control or treatment groups after 15 days of EG challenge. Scale bar: 100 µm. (E) Analysis of CaOx accumulation in representative kidneys of animals from control or treatment groups after 15 days of EG challenge. Scale bar: 200 µm. Kruskal-Wallis statistical test was used to compare the groups in each day. *p < 0.05. ns, not significant.

The high reduction of LDH protein is translated into an outstanding long-term therapeutic effect in both PH1 and PH3 animal models, in line with previous results observed with siRNAs targeting LDH.[18] Our results clearly showed that urine oxalate levels and oxalate crystal formation were significantly reduced, with a clear improvement in additional indicators of the disease, like the reduced weight loss caused by renal failure induced by the oxalate overproduction. These results are further substantiated by the fact that treated animals were fully protected against metabolic challenge with oxalate precursors (EG and HP). Moreover, as previously observed for GO,[26] the efficacy of CRIPSR/Cas9-mediated LDH inhibition can be observed as soon as 8 weeks after vector administration, although in general, more robust and homogeneous results were observed at longer times, including higher indel frequencies, reduced *Ldha* mRNA expression and urine oxalate levels after challenge, and lower weight loss. Interestingly, the increase of vector dose (up to 10^{14} vg/kg) does not provide significant improvements in the therapeutic efficacy. This is probably related to the high efficiency of liver transduction achieved with AAV8, as supported by the fact that doses of 5×10^{12} vg/kg infect >95% of the hepatocytes.[9] Again, similar to our observations inhibiting GO,[26] our therapeutic approach targeting LDH was safe, because treated animals presented normal liver histology without elevation of liver transaminases.

An important consideration, in contrast with siRNA-based therapies, is that CRISPR-Cas9 approaches, based on AAV vectors, will continuously express Cas9, increasing the probability of non-specific modifications of the genome. Improved delivery approaches with more translational potential, like the use of nanoparticles for the delivery of RNP or mRNA/sgRNA complexes,[40,41] which are currently under development, would contribute to reduce these risks. However, several studies have shown that mutations in non-target regions attributable to Cas9 are rare.[42,43] In our study, we did not observe cleavage in predicted off-target regions after deep sequencing in animals treated for at least 6 months, while on-target site was efficiently edited only in the liver. Moreover, insertions of AAV vector into sgRNA-targeted regions, although detectable, were low compared with recent publications,[32] suggesting that these events may be highly dependent on the sgRNA design and/or the targeted locus. Results regarding unspecific cleavage are in accordance with our previous studies targeting GO,[26] as well as with other studies using CRISPR-Cas9 systems in the liver and in other tissues like the muscle.[44–46] Even in the case of nonspecific cleavage events, several alternatives have been proposed to decrease off-target modifications, including improved sgRNA design algorithms that allow the selection of guides with reduced off-target potential.[47]

In summary, in this work we have demonstrated that targeting LDH using CRISPR-Cas9 systems delivered by AAV vectors results in an extraordinary therapeutic effect in both PH1 and PH3 mice. Together with our previous results targeting GO,[26] our data provide evidence for the use of CRIPSR/Cas9 approaches as a promising efficient and

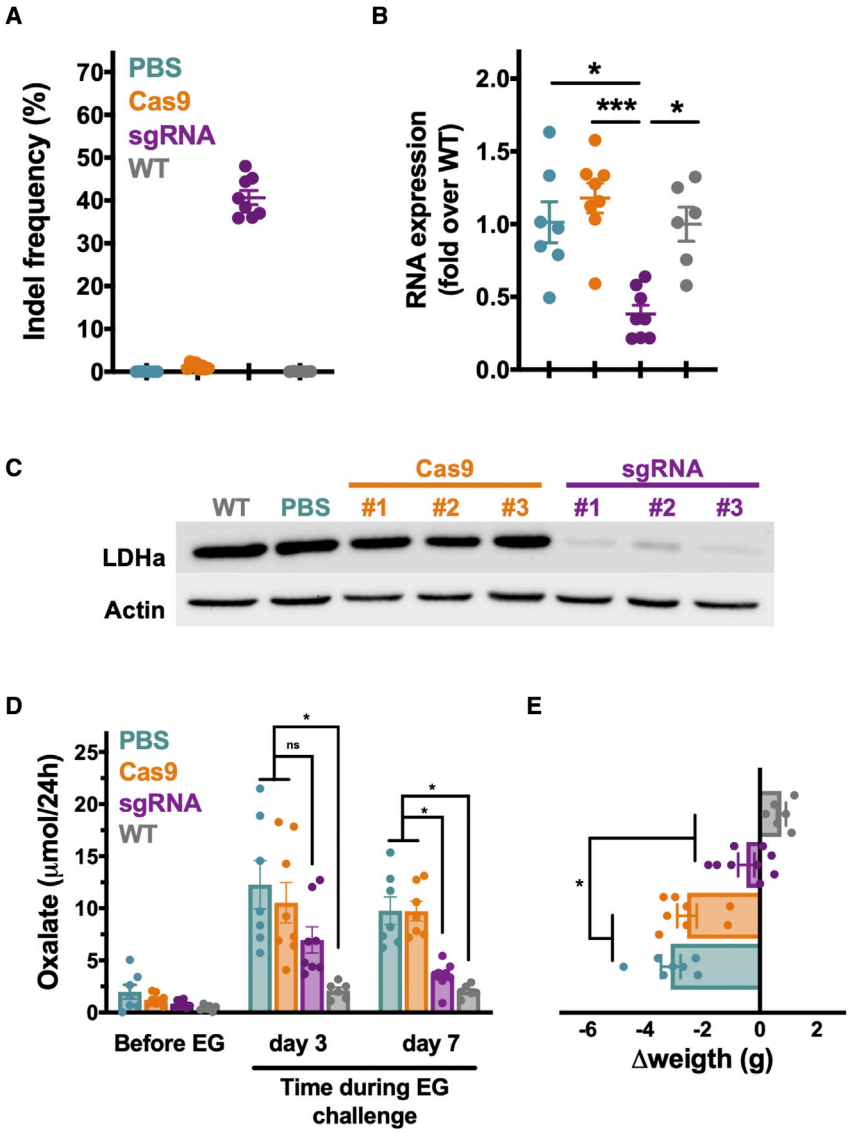

Figure 4. Therapeutic efficacy of CRISPR-Cas9-mediated LDH inhibition in *Hoga1*$^{-/-}$ mice

Analysis performed in 10- to 14-week-old PH3 animals 6 months after treatment with PBS (n = 7), Cas9 (n = 8), and sgRNA (n = 8) and in WT animals (n = 6). (A) Editing efficiency measured by TIDE. (B) Quantification of *Ldha* mRNA expression by quantitative real-time PCR. (C) WB analysis of LDH protein levels in representative WT and PH3 animals treated with PBS, Cas9, and sgRNA. Actin was used as loading control. (D) Quantification of urine oxalate levels (µmol/24 h) before and on days 3 and 7 of HP challenge in the different groups of treatment. (E) Weight change of the animals after 1 week of HP challenge in the different groups of treatment. Kruskal-Wallis statistical test was used to compare the groups in each day. *p < 0.05, ***p < 0.001.

safe therapeutic strategy for PH patients, which should be further corroborated in more clinically relevant approaches and disease models. These results also support the use of CRISPR-Cas9-based strategies for the inhibition of specific genes in the liver in other inherited metabolic diseases.[48,49]

MATERIALS AND METHODS

gRNA design and *in vitro* evaluation

sgRNAs targeting the *Ldha* gene were designed and selected as described previsouly[26] using Benchling software (https://www.benchling.com). The sgRNAs are shown in Table S1. *In vitro* cleavage efficiency was evaluated using RNP complex in Hepa1–6 (ATCC CRL-1830) and AML12 (ATCC CRL-2254) mouse hepatic cell lines. SaCas9 protein was purchased from ABM (#K144) and combined with *in-vitro*-transcribed (IVT) sgRNAs generated using Genecraft-R classic CRISPR sgRNA synthesis kit (ABM) according to the manufacturers' instructions. Cell lines were electroporated with 21 µg of RNP (9 µg of SaCas9 and 12 µg of IVT sgRNA) using the SF Cell Line 4D-Nucleofector X Kit and the CM-138 program on a 4D-Nucleofector System (Lonza). Hepa1–6 cells were cultured in DMEM supplemented with 10% FBS, 2 mM L-glutamine, and 100 UI/mL P/S. AML12 cells were cultured in DMEM:F12 supplemented with 10% FBS, 10 µg/mL insulin, 5.5 µg/mL transferrin, 5 ng/mL selenium, 40 ng/mL dexamethasone, 2 mM L-glutamine, and 100 UI/mL P/S. All cell culture reagents were purchased form Gibco.

CRISPR-Cas9 vectors and AAV8 vector production

The plasmid pX602-AAV-TBG:NLS-SaCas9-NLS-HA-OLLAS-bGHpA; U6:BsaI-sgRNA containing SaCas9 under TBG promoter, the U6 promoter to express the sgRNA and ITR sequences for AAV production, was a gift from Feng Zhang (plasmid #61593; Addgene).[50] sgRNAs were cloned, and serotype 8 AAV vectors were produced as described previously.[26] AAV titration was performed using viral DNA isolated using the High Pure Viral Nucleic Acid kit (Roche Applied Science). Viral titers (vg/mL) were determined by quantitative real-time PCR (Applied Biosystems) using SaCas9-specific primers (Table S5).

Animal experiments

All procedures involving animal experimentation were approved by the Ethics Committee of the University of Navarra according to European Guidelines. *Agxt1*$^{-/-}$ mice (B6.129SvAgxt^{tm1Ull}) and *Hoga1*$^{-/-}$ (B6.129X1-Hoga1$^{tm2e(KOMP)Wtsi}$) mice were bred and maintained in a pathogen-free facility with free access to standard chow and water. *Agxt1*$^{-/-}$ and *Hoga1*$^{-/-}$ mice were

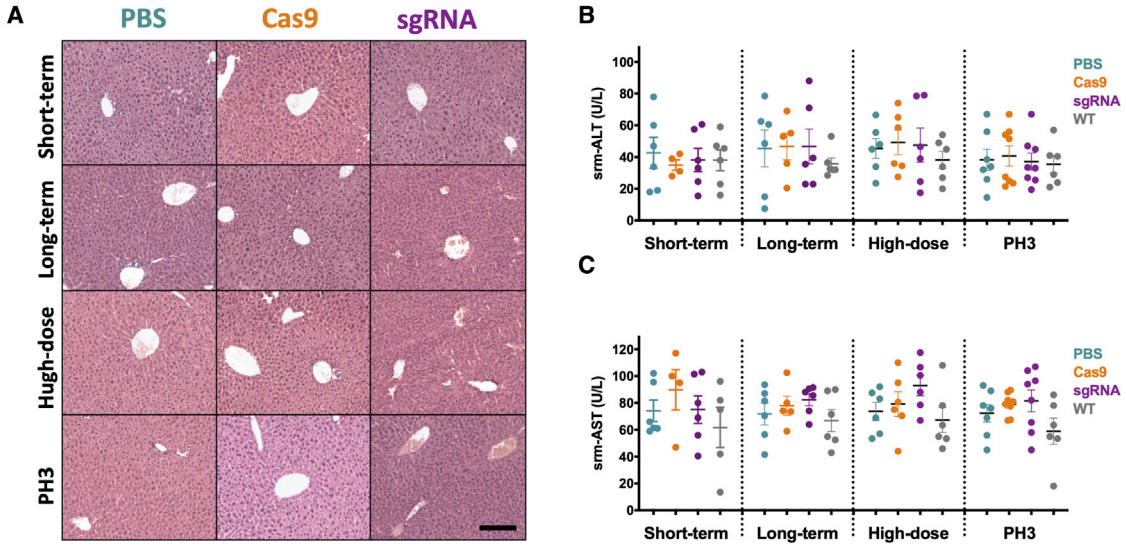

Figure 5. Safety of CRISPR-Cas9-mediated LDH inhibition

(A) Representative hematoxylin and eosin staining of liver sections from 10- to 14-week-old PH1 and PH3 animals sacrificed 8 weeks (short term and high dose) or 6 months (long term and PH3) after treatment. (B) Serum ALT (U/L) levels in the different groups of treatment. (C) Serum AST (U/L) levels in the different groups of treatment. Kruskal-Wallis test revealed no significant differences between groups. Scale bar: 200 μm.

genotyped as described previously,[29] using specific primers (Table S5). Age-matched C57BL/6J mice (Harlan laboratories) were used as control animals. AAV vectors (5×10^{12} vg/kg) were intravenously administered to 10- to 14-week-old *Agxt1*$^{-/-}$ or *Hoga1*$^{-/-}$ male animals. For high-dose experiments, animals were administered 10^{14} vg/kg by the same route. For challenge studies, *Agxt1*$^{-/-}$ animals were given free access to drinking water containing 0.5% (v/v) EG. *Hoga1*$^{-/-}$ animals were subjected to HP feeding by either free access to a custom animal diet containing 1% HP, free access to drinking water containing 0.25 M HP, or a single gavage feeding with 0.5 M HP. Collection of 24-h urine samples and monitorization of water intake during the challenge were performed in mice individualized in metabolic cages. Urine, serum, and tissue samples (liver, heart, kidney, lung, and spleen) were collected as described previously.[26]

Extraction of gDNA and quantification of indels

The NucleoSpin Tissue DNA extraction kit (Macherey-Nagel) was used for genomic DNA extraction from tissue sections according to the manufacturer's instructions. Indel percentage was calculated using TIDE webtool (https://tide.nki.nl).[27]

Analysis of the on-target and off-target cleavage

Prediction of top 5 off-target candidates for the selected sgRNA was determined using Benchling software (https://www.benchling.com) (Table S2). NGS analysis was performed as described previously.[26] Briefly, gDNA was amplified using specific primers (Table S5) to generate Illumina amplicons with specific barcodes for each sample by nested PCR. The final library was sequenced on Illumina MiSeq (2×250 bp paired end) at >25,000× coverage. Reads were aligned to the reference genome (GRCm38/mm10) using Burrows-Wheeler Aligner (BWA), and indels were determined using CrispRVariants R-based toolkit[51] as described previously.[26] To analyze insertions containing AAV sequences, we aligned reads to the reference genome containing the AAV vector sequence as described previously.[32]

Viral genome copies and gene expression

Viral genome copies were quantified by quantitative real-time PCR from gDNA using SaCas9-specific primers (Table S5) as described previously.[26] RNA was isolated using TRIzol (Life Technology) and *Ldha*, and SaCas9 gene expression was analyzed by quantitative real-time PCR as described previously.[26] Data were normalized to GAPDH levels.

Western blot and immunohistochemistry

Western blot for LDH detection was performed as described previously[26] using a rabbit anti-LDH antibody (ab47010; Abcam) at a 1:5,000 dilution. Immunohistochemical detection of LDHA was performed in paraffin liver sections as described previously[18] using a rabbit polyclonal anti-LDHA antibody (1:50 dilution; Cell Signaling Technology, Danvers, MA, USA).

Urine oxalate/glycolate measurement and serum biochemistry

Urine oxalate levels were measured using the Oxalate kit (Trinity Biotech) according to the manufacturer's instructions. Glycolate concentration was measured in a colorimetric assay using recombinant GO enzyme as described previously.[26] Peripheral blood samples were collected at the indicated time points, and serum ALT and AST levels were quantified as described previously.[26]

Histological analysis of kidney and hematoxylin and eosin staining

Hematoxylin and eosin staining was performed in paraffin liver and kidney sections as described previously.[26] Kidney sections were analyzed under dark field to count oxalate deposits in three cortical areas using a microscope (Leica DMLB) fitted with polarization filters.

Statistics

Results are presented as mean ± standard error of the mean (SEM) of at least four mice per group at each time point to ensure reproducibility. Sample sizes are noted in the figure legends. Graphs and statistical analyses were performed using GraphPad Prism 9.0.0. Kruskal-Wallis test with Dunn's post-test or Friedman test was used to analyze differences between groups. Mann-Whitney test was used for individual comparisons. The p values <0.05 were considered significant.

Data availability

All authors declare that data are available within the article or the supplemental information files, or are available in a public database. Sequencing raw data (fastq files) have been deposited in Sequence Read Archive (SRA; BioProject PRJNA701658) and are available at https://dataview.ncbi.nlm.nih.gov/object/24175283.

SUPPLEMENTAL INFORMATION

Supplemental information can be found online at https://doi.org/10.1016/j.omtm.2022.03.006.

ACKNOWLEDGMENTS

This study was supported by the Instituto de Salud Carlos III co-financed by European Regional Development Fund-FEDER "A way to make Europe" (PI16/00150 and PI19/00922), ERA-NET E-Rare 3 research program JTC ERAdicatPH (AC15/00036), Red de Terapia Celular TERCEL (RD16/0011/0005), Red Española de Terapias Avanzadas TERAV (RD21/0017/0009), Centro de Investigación Biomédica en Red de Cáncer CIBERONC (CB16/12/00489), and Oxalosis and Hyperoxaluria Foundation. P.R.-M. was supported by an FPU grant (FPU19/06160) from Ministerio de Universidades.

AUTHOR CONTRIBUTIONS

Conceptualization, F.P. and J.R.R.-M.; methodology, P.S.M.-U., A.V.-Z., and M.E.C.-C.; formal analysis, R.M.-T., A.M.-M., E.S., and J.R.R.-M.; investigation, R.M.-T., A.M.-M., S.R.-D., N.Z.-L., and P.R.-M.; resources, E.S.; writing – original draft, J.R.R.-M.; writing – review & editing, E.S., F.P., and J.R.R.-M.; supervision: F.P. and J.R.R.-M.; funding acquisition, F.P. and J.R.R.-M.

DECLARATION OF INTERESTS

E.S. holds shares of Orfan Biotech. The rest of the authors declare no competing interests.

REFERENCES

1. Salido, E., Pey, A.L., Rodriguez, R., and Lorenzo, V. (2012). Primary hyperoxalurias: disorders of glyoxylate detoxification. Biochim. Biophys. Acta - Mol. Basis Dis. *1822*, 1453–1464.
2. Cochat, P., and Rumsby, G. (2013). Primary hyperoxaluria. N. Engl. J. Med. *369*, 649–658.
3. Danpure, C.J., and Jennings, P.R. (1986). Peroxisomal alanine:glyoxylate aminotransferase deficiency in primary hyperoxaluria type I. FEBS Lett. *201*, 20–24.
4. Kemper, M.J., Conrad, S., and Müller-Wiefel, D.E. (1997). Primary hyperoxaluria type 2. Eur. J. Pediatr. *156*, 509–512.
5. Belostotsky, R., Seboun, E., Idelson, G.H., Milliner, D.S., Becker-Cohen, R., Rinat, C., Monico, C.G., Feinstein, S., Ben-Shalom, E., Magen, D., et al. (2010). Mutations in DHDPSL are responsible for primary hyperoxaluria type III. Am. J. Hum. Genet. *87*, 392–399.
6. Fargue, S., Harambat, J., Gagnadoux, M.F., Tsimaratos, M., Janssen, F., Llanas, B., Berthélémé, J.P., Boudailliez, B., Champion, G., Guyot, C., et al. (2009). Effect of conservative treatment on the renal outcome of children with primary hyperoxaluria type 1. Kidney Int. *76*, 767–773.
7. Beck, B.B., Hoyer-Kuhn, H., Göbel, H., Habbig, S., and Hoppe, B. (2013). Hyperoxaluria and systemic oxalosis: an update on current therapy and future directions. Expert Opin. Invest. Drugs *22*, 117–129.
8. Jiang, J., Salido, E.C., Guha, C., Wang, X., Moitra, R., Liu, L., Roy-Chowdhury, J., and Roy-Chowdhury, N. (2008). Correction of hyperoxaluria by liver repopulation with hepatocytes in a mouse model of primary hyperoxaluria type-1. Transplantation *85*, 1253–1260.
9. Salido, E., Rodriguez-Pena, M., Santana, A., Beattie, S.G., Petry, H., and Torres, A. (2011). Phenotypic correction of a mouse model for primary hyperoxaluria with adeno-associated virus gene transfer. Mol. Ther. *19*, 870–875.
10. Miyata, N., Steffen, J., Johnson, M.E., Fargue, S., Danpure, C.J., and Koehler, C.M. (2014). Pharmacologic rescue of an enzyme-trafficking defect in primary hyperoxaluria 1. Proc. Natl. Acad. Sci. U S A *111*, 14406–14411.
11. Milliner, D., Hoppe, B., and Groothoff, J. (2018). A randomised Phase II/III study to evaluate the efficacy and safety of orally administered Oxalobacter formigenes to treat primary hyperoxaluria. Urolithiasis *46*, 313–323.
12. Dutta, C., Avitahl-Curtis, N., Pursell, N., Larsson Cohen, M., Holmes, B., Diwanji, R., Zhou, W., Apponi, L., Koser, M., Ying, B., et al. (2016). Inhibition of glycolate oxidase with dicer-substrate siRNA reduces calcium oxalate deposition in a mouse model of primary hyperoxaluria type 1. Mol. Ther. *24*, 770–778.
13. Liebow, A., Li, X., Racie, T., Hettinger, J., Bettencourt, B.R., Najafian, N., Haslett, P., Fitzgerald, K., Holmes, R.P., Erbe, D., et al. (2017). An investigational RNAi therapeutic targeting glycolate oxidase reduces oxalate production in models of primary hyperoxaluria. J. Am. Soc. Nephrol. *28*, 494–503.
14. Garrelfs, S.F., Frishberg, Y., Hulton, S.A., Koren, M.J., O'Riordan, W.D., Cochat, P., Deschênes, G., Shasha-Lavsky, H., Saland, J.M., van't Hoff, W.G., et al. (2021). Lumasiran, an RNAi therapeutic for primary hyperoxaluria type 1. N. Engl. J. Med. *384*, 1216–1226.
15. Mdluli, K., Booth, M.P.S., Brady, R.L., and Rumsby, G. (2005). A preliminary account of the properties of recombinant human Glyoxylate reductase (GRHPR), LDHA and LDHB with glyoxylate, and their potential roles in its metabolism. Biochim. Biophys. Acta - Proteins Proteomics *1753*, 209–216.
16. Markert, C.L., Shaklee, J.B., and Whitt, G.S. (1975). Evolution of a gene: multiple genes for LDH isozymes provide a model of the evolution of gene structure, function, and regulation. Science *189*, 102–114.
17. Ariceta, G., Barrios, K., Brown, B.D., Hoppe, B., Rosskamp, R., and Langman, C.B. (2021). Hepatic lactate dehydrogenase A: an RNA interference target for the treatment of all known types of primary hyperoxaluria. Kidney Int. Rep. *6*, 1088–1098.
18. Lai, C., Pursell, N., Gierut, J., Saxena, U., Zhou, W., Dills, M., Diwanji, R., Dutta, C., Koser, M., Nazef, N., et al. (2018). Specific inhibition of hepatic lactate dehydrogenase reduces oxalate production in mouse models of primary hyperoxaluria. Mol. Ther. *26*, 1983–1995.
19. Hoppe, B., Koch, A., Cochat, P., Garrelfs, S.F., Baum, M.A., Groothoff, J.W., Lipkin, G., Coenen, M., Schalk, G., Amrite, A., et al. (2021). Safety, pharmacodynamics, and

exposure-response modeling results from a first in human phase 1 study of nedosiran in primary hyperoxaluria. Kidney Int. *101*, 626–634.

20. Gaj, T., Gersbach, C.A., and Barbas, C.F. (2013). ZFN, TALEN, and CRISPR/Cas-based methods for genome engineering. Trends Biotechnol. *31*, 397–405.
21. Cox, D.B.T., Platt, R.J., and Zhang, F. (2015). Therapeutic genome editing: prospects and challenges. Nat. Med. *21*, 121–131.
22. Komor, A.C., Badran, A.H., and Liu, D.R. (2017). CRISPR-based technologies for the manipulation of eukaryotic genomes. Cell *168*, 20–36.
23. Lu, Y., Xue, J., Deng, T., Zhou, X., Yu, K., Deng, L., Huang, M., Yi, X., Liang, M., Wang, Y., et al. (2020). Safety and feasibility of CRISPR-edited T cells in patients with refractory non-small-cell lung cancer. Nat. Med. *26*, 732–740.
24. Stadtmauer, E.A., Fraietta, J.A., Davis, M.M., Cohen, A.D., Weber, K.L., Lancaster, E., Mangan, P.A., Kulikovskaya, I., Gupta, M., Chen, F., et al. (2020). CRISPR-engineered T cells in patients with refractory cancer. Science *367*, 1–20.
25. Frangoul, H., Altshuler, D., Cappellini, M.D., Chen, Y.-S., Domm, J., Eustace, B.K., Foell, J., de la Fuente, J., Grupp, S., Handgretinger, R., et al. (2020). CRISPR-Cas9 gene editing for sickle cell disease and β-thalassemia. N. Engl. J. Med. *384*, 252–260.
26. Zabaleta, N., Barberia, M., Martin-Higueras, C., Zapata-Linares, N., Betancor, I., Rodriguez, S., Martinez-Turrillas, R., Torella, L., Vales, A., Olagüe, C., et al. (2018). CRISPR/Cas9-mediated glycolate oxidase disruption is an efficacious and safe treatment for primary hyperoxaluria type I. Nat. Commun. *9*, 5454.
27. Brinkman, E.K., Chen, T., Amendola, M., and Van Steensel, B. (2014). Easy quantitative assessment of genome editing by sequence trace decomposition. Nucleic Acids Res. *42*, 1–8.
28. Yan, Z., Yan, H., and Ou, H. (2012). Human thyroxine binding globulin (TBG) promoter directs efficient and sustaining transgene expression in liver-specific pattern. Gene *506*, 289–294.
29. Salido, E.C., Li, X.M., Lu, Y., Wang, X., Santana, A., Roy-Chowdhury, N., Torres, A., Shapiro, L.J., and Roy-Chowdhury, J. (2006). Alanine-glyoxylate aminotransferase-deficient mice, a model for primary hyperoxaluria that responds to adenoviral gene transfer. Proc. Natl. Acad. Sci. U S A *103*, 18249–18254.
30. Li, X., Knight, J., Todd Lowther, W., and Holmes, R.P. (2015). Hydroxyproline metabolism in a mouse model of primary hyperoxaluria type 3. Biochim. Biophys. Acta - Mol. Basis Dis. *1852*, 2700–2705.
31. Fargue, S., Milliner, D.S., Knight, J., Olson, J.B., Lowther, W.T., and Holmes, R.P. (2018). Hydroxyproline metabolism and oxalate synthesis in primary hyperoxaluria. J. Am. Soc. Nephrol. *29*, 1615–1623.
32. Hanlon, K.S., Kleinstiver, B.P., Garcia, S.P., Zaborowski, M.P., Volak, A., Spirig, S.E., Muller, A., Sousa, A.A., Tsai, S.Q., Bengtsson, N.E., et al. (2019). High levels of AAV vector integration into CRISPR-induced DNA breaks. Nat. Commun. *10*, 4439.
33. Li, H., Haurigot, V., Doyon, Y., Li, T., Wong, S.Y., Bhagwat, A.S., Malani, N., Anguela, X.M., Sharma, R., Ivanciu, L., et al. (2011). In vivo genome editing restores haemostasis in a mouse model of haemophilia. Nature *475*, 217–221.
34. Nelson, C.E., Hakim, C.H., Ousterout, D.G., Thakore, P.I., Moreb, E.A., Rivera, R.M.C., Madhavan, S., Pan, X., Ran, F.A., Yan, W.X., et al. (2016). In Vivo genome editing improves muscle function in a mouse model of Duchenne muscular dystrophy. Science *351*, 403–407.
35. Pankowicz, F.P., Barzi, M., Legras, X., Hubert, L., Mi, T., Tomolonis, J.A., Ravishankar, M., Sun, Q., Yang, D., Borowiak, M., et al. (2016). Reprogramming metabolic pathways in vivo with CRISPR/Cas9 genome editing to treat hereditary tyrosinaemia. Nat. Commun. *7*, 12642.
36. Jarrett, K.E., Lee, C.M., Yeh, Y.H., Hsu, R.H., Gupta, R., Zhang, M., Rodriguez, P.J., Lee, C.S., Gillard, B.K., Bissig, K.D., et al. (2017). Somatic genome editing with CRISPR/Cas9 generates and corrects a metabolic disease. Sci. Rep. *7*, 1–12.
37. Srifa, W., Kosaric, N., Amorin, A., Jadi, O., Park, Y., Mantri, S., Camarena, J., Gurtner, G.C., and Porteus, M. (2020). Cas9-AAV6-engineered human mesenchymal stromal cells improved cutaneous wound healing in diabetic mice. Nat. Commun. *11*, 2470.
38. Zhao, H., Li, Y., He, L., Pu, W., Yu, W., Li, Y., Wu, Y.T., Xu, C., Wei, Y., DIng, Q., et al. (2020). In vivo AAV-CRISPR/Cas9-Mediated gene editing ameliorates atherosclerosis in familial hypercholesterolemia. Circulation *141*, 67–79.
39. Zheng, R., Fang, X., Chen, X., Huang, Y., Xu, G., He, L., Li, Y., Niu, X., Yang, L., Wang, L., et al. (2020). Knockdown of lactate dehydrogenase by adeno-associated virus-delivered CRISPR/Cas9 system alleviates primary hyperoxaluria type 1. Clin. Translational Med. *10*, e261.
40. Mangeot, P.E., Risson, V., Fusil, F., Marnef, A., Laurent, E., Blin, J., Mournetas, V., Massouridès, E., Sohier, T.J.M., Corbin, A., et al. (2019). Genome editing in primary cells and in vivo using viral-derived Nanoblades loaded with Cas9-sgRNA ribonucleoproteins. Nat. Commun. *10*, 1–15.
41. Finn, J.D., Smith, A.R., Patel, M.C., Shaw, L., Youniss, M.R., van Heteren, J., Dirstine, T., Ciullo, C., Lescarbeau, R., Seitzer, J., et al. (2018). A single administration of CRISPR/Cas9 lipid nanoparticles achieves robust and persistent in vivo genome editing. Cell Rep. *22*, 2227–2235.
42. Iyer, V., Shen, B., Zhang, W., Hodgkins, A., Keane, T., Huang, X., and Skarnes, W.C. (2015). Off-target mutations are rare in Cas9-modified mice. Nat. Methods *12*, 479.
43. Sang-Tae, K. (2017). Questioning unexpected CRISPR off-target mutations in vivo. Preprint at biorxiv, 2017/06/30/157925.
44. Yin, H., Song, C.-Q., Dorkin, J.R., Zhu, L.J., Li, Y., Wu, Q., Park, A., Yang, J., Suresh, S., Bizhanova, A., et al. (2016). Therapeutic genome editing by combined viral and non-viral delivery of CRISPR system components in vivo. Nat. Biotechnol. *34*, 328–333.
45. Yang, Y., Wang, L., Bell, P., McMenamin, D., He, Z., White, J., Yu, H., Xu, C., Morizono, H., Musunuru, K., et al. (2016). A dual AAV system enables the Cas9-mediated correction of a metabolic liver disease in newborn mice. Nat. Biotechnol. *34*, 334–338.
46. Tabebordbar, M., Zhu, K., Cheng, J.K.W., Chew, W.L., Widrick, J.J., Yan, W.X., Maesner, C., Wu, E.Y., Xiao, R., Ran, F.A., et al. (2016). In Vivo gene editing in dystrophic mouse muscle and muscle stem cells. Science *351*, 407–411.
47. Doench, J.G., Fusi, N., Sullender, M., Hegde, M., Vaimberg, E.W., Donovan, K.F., Smith, I., Tothova, Z., Wilen, C., Orchard, R., et al. (2016). Optimized sgRNA design to maximize activity and minimize off-target effects of CRISPR-Cas9. Nat. Biotechnol. *34*, 184–191.
48. Clayton, N.P., Nelson, C.A., Weeden, T., Taylor, K.M., Moreland, R.J., Scheule, R.K., Phillips, L., Leger, A.J., Cheng, S.H., and Wentworth, B.M. (2014). Antisense oligonucleotide-mediated suppression of muscle glycogen synthase 1 synthesis as an approach for substrate reduction therapy of pompe disease. Mol. Ther. - Nucleic Acids *3*, e206.
49. Lamanna, W.C., Lawrence, R., Sarrazin, S., Lameda-Diaz, C., Gordts, P.L.S.M., Moremen, K.W., and Esko, J.D. (2012). A genetic model of substrate reduction therapy for mucopolysaccharidosis. J. Biol. Chem. *287*, 36283–36290.
50. Ran, F.A., Cong, L., Yan, W.X., Scott, D.A., Gootenberg, J.S., Kriz, A.J., Zetsche, B., Shalem, O., Wu, X., Makarova, K.S., et al. (2015). In vivo genome editing using Staphylococcus aureus Cas9. Nature *520*, 186–191.
51. Lindsay, H., Burger, A., Biyong, B., Felker, A., Hess, C., Zaugg, J., Chiavacci, E., Anders, C., Jinek, M., Mosimann, C., et al. (2016). CrispRVariants charts the mutation spectrum of genome engineering experiments. Nat. Biotechnol. *34*, 701–702.